

Dependence of exciton energy on dot size in GaN/AlN quantum dots

D. P. Williams,^{1,*} A. D. Andreev,² and E. P. O'Reilly¹

¹*Tyndall National Institute, Lee Maltings, Cork, Ireland*

²*Advanced Technology Institute, University of Surrey, Guildford GU2 7XH, United Kingdom*

(Received 27 January 2006; revised manuscript received 7 April 2006; published 6 June 2006)

Using previously derived analytical expressions for the polarization field in nitride quantum dots (QDs), we show that the potential in the growth direction can be approximated as linear in such dots, and that the slope of this linear potential depends only on the aspect ratio (height/radius) of the dot. We demonstrate how the large polarization field leads to a linear dependence of the exciton energy on dot size, provided the aspect ratio of the dot is conserved while the size is varied. We also present a useful analytical approximation for the electron and hole wave functions in nitride QDs in terms of Airy functions, which compares well with the solutions of a numerical computation. We note that the disagreement concerning the sign of the shear piezoelectric coefficient e_{15} leads to a significant uncertainty in the calculated potential.

DOI: [10.1103/PhysRevB.73.241301](https://doi.org/10.1103/PhysRevB.73.241301)

PACS number(s): 73.21.La, 77.65.Ly

Quantum dot (QD) structures are currently of great interest due to their advantages over quantum wells and wires, in that they confine charge in all three dimensions, promising more efficient lasers and optical amplifiers as well as possible applications for memory storage and quantum computing. Nitride-based QDs are of particular interest, since the large built-in electric fields in these structures means they can be potentially engineered to emit anywhere from the infrared to the ultraviolet simply by varying the dot size and composition. These large fields arise from both the spontaneous polarization present in the wurtzite crystal structure of the nitrides, and the strain-induced polarization associated with the large piezoelectric constants and lattice mismatch of the materials. Previous investigations on arsenide-based systems, which do not exhibit these large fields, have revealed a rather complex dependence of the ground-state exciton emission energy on dot size.^{1–3} In contrast, the large built-in fields in nitride QDs dominate the behaviour of confined electrons and holes, resulting in a near-linear dependence of exciton energy on dot size.⁴ In this paper, we use a simple analytical model together with our previously derived expressions for the polarization potential to demonstrate explicitly that the source of this dependence is the built-in electric field along the growth (z) axis. We will show that the polarization field along the dot axis is approximately constant, and this leads to a linear variation of the exciton recombination energy with dot size, provided the aspect ratio is conserved as the dot size is varied. In addition, we present an approximate solution for the electron and hole wave functions in the z direction involving Airy functions, which gives energies and wave functions very close to those of a full numerical simulation. This allows the estimation of electron-hole overlap, which is important for quantities such as exciton lifetime and oscillator strength.

Our previous work^{5,6} on built-in polarization fields in nitride QDs has shown that the field in the z direction [which we take to be the (0001) growth direction] has the most significant effect on the confinement potential, reaching 6–8 MV/cm in GaN/AlN QDs, with the in-plane field of ~ 1 MV/cm providing additional lateral confinement. We therefore begin our approximation by separating the potential

into a radial part and an axial (z direction) part. First, the radial polarization potential is approximated by a harmonic oscillator potential $\frac{1}{2}kr^2$, with the value of k given by the second derivative with respect to x of the potential evaluated at $r=0$, $\partial_x^2\varphi(z)$, for which we have previously derived analytical expressions.⁶ It remains to decide at what value of z this should be evaluated—this will be discussed later. In the case of a cylindrical dot, this approximation is usually accurate to within 1% out to about half the radius of the dot, in the range of realistic dot dimensions. However, for very small dots and dots with very large aspect ratios the potential step at the interface between the materials becomes increasingly important and the lateral potential begins to take on a quantum well nature. The approximation is also reasonably accurate for truncated cone dots as long as the side angle of the dot is not too small and the dot does not get too narrow near the top. This approach then gives a lateral confinement energy of

$$E_r = \hbar \sqrt{\frac{k}{m^*}} \quad (1)$$

where m^* is the effective mass of the carrier being considered (electron or hole).

For the axial part, the potential along the central z axis of a cylindrical QD with radius R and height h with its base centered on the origin is given by⁶

$$\varphi(z) = JI_1 + \left(K + \frac{P_{QD} - P_M}{4\pi\epsilon_r\epsilon_0} \right) I_2 \quad (2)$$

where

$$I_1 = 2\pi \left(\frac{z^2}{\sqrt{R^2 + z^2}} - z \operatorname{sgn}(z) - \frac{(z-h)^2}{\sqrt{R^2 + (z-h)^2}} + (z-h) \operatorname{sgn}(z-h) \right), \quad (3)$$

$$I_2 = 2\pi[-\sqrt{R^2 + z^2} + z \operatorname{sgn}(z) + \sqrt{R^2 + (z-h)^2} - (z-h)\operatorname{sgn}(z-h)]. \quad (4)$$

P_{QD} and P_M are the spontaneous polarization constants of the QD and matrix materials, respectively, ϵ_r is the relative permittivity of the QD material, and J and K are constants given by

$$J = \frac{-\epsilon_0(1+\nu)(2e_{15} - e_{33} + e_{31})}{8\pi\epsilon_r\epsilon_0(1-\nu)},$$

$$K = \frac{\epsilon_0}{8\pi\epsilon_r\epsilon_0} \left(4e_{31} + 2e_{33} - \frac{1+\nu}{1-\nu}(2e_{15} + e_{31} + e_{33}) \right)$$

where ϵ_0 is the isotropic misfit strain, ν is Poisson's ratio, and e_{ij} are the piezoelectric constants. A number of assumptions were made in the derivation of these expressions, including isotropic elastic constants and the same elastic, piezoelectric, and dielectric constants in both materials; see Ref. 6 for a full discussion.

We use the above expressions to calculate the variation of the conduction and valence band energy along the z axis, as shown in Fig. 1 (solid line). For convenience, we do not consider a wetting layer. However, this can be easily included if required and does not change our overall conclusions. In order to obtain an analytical expression for the axial confinement energy E_z , we approximate the calculated potential by a triangular well with one finite potential step (dashed line in Fig. 1), which we can then solve analytically. To obtain the slope of this approximate potential, we make a series expansion of Eqs. (3) and (4) in z about the point $z = h/2$ and take only the linear terms, which gives

$$I_1 \approx 4\pi \left(z - \frac{h}{2} \right) \left(-1 + \frac{2f}{\sqrt{4+f^2}} - \frac{f^3}{(4+f^2)^{3/2}} \right), \quad (5)$$

$$I_2 \approx 4\pi \left(z - \frac{h}{2} \right) \left(1 - \frac{f}{\sqrt{4+f^2}} \right), \quad (6)$$

where $f = h/R$ is the ratio of the dot height to radius. The slope F of the potential can then be obtained using the expressions (2), (5), and (6). It is important to note that the size of the dot can be varied without changing F , provided the aspect ratio f is conserved. The validity of this linear approximation of the potential for a cylindrical dot can be gauged from the maximum error, which occurs at $z=0$ and $z=h$. With the material parameters from Ref. 7 and taking $\epsilon_r=9.6$, this error is less than 1% for $f \leq 0.45$, increasing to 3.5% at $f=0.7$. In the case of truncated cone QDs, expressions similar to (3) and (4), but more complicated, can be used to obtain the equivalent expression for F .⁶ Alternatively, a cylindrical dot with the same height and volume as the truncated cone can be used to give a reasonable estimate for F .

We note also that there is a large degree of uncertainty in many of the material parameters for the nitrides, and the choice of parameters can have a significant effect on the potential obtained. This is particularly noticeable in the case of quantum dots, since the expressions for a QD involve e_{15} ,

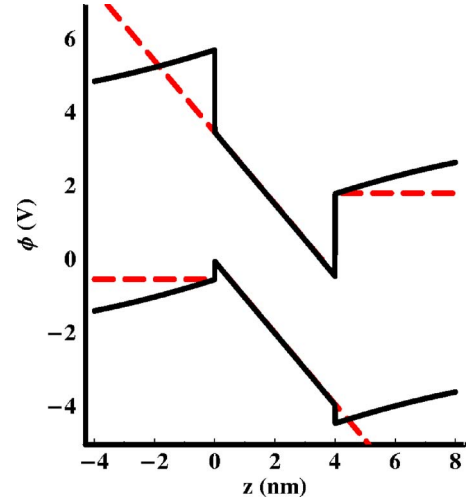


FIG. 1. (Color online) Conduction and valence band edges through the center of a GaN/AlN cylindrical QD with radius 10.5 nm and height 4 nm. Solid line, numerically calculated band edges. Dashed line, approximate band edges using a linear polarization potential and a single finite potential step. Material parameters taken from Ref. 7.

while those for a quantum well do not.⁸ There is conflicting evidence not only for the magnitude of e_{15} , but also for its sign, with Refs. 9 and 10 deriving a positive sign while Refs. 11 and 12 derive a negative sign. In this paper we use the parameters from Ref. 7, which give a positive value of e_{15} . In previous work^{5,13} we have used a different set of parameters with a negative e_{15} , which give a significantly smaller potential variation than that calculated here, mostly due to the change in sign of e_{15} . If we expand I_1 and I_2 in a power series in f and then retain terms up to linear in f , the contribution $\varphi_{15}(z)$ due to the terms involving e_{15} is given by

$$\varphi_{15}(z) = \frac{\epsilon_0 z}{2\epsilon_r\epsilon_0} \frac{1+\nu}{1-\nu} e_{15} f. \quad (7)$$

This term is zero in a quantum well ($f=0$) but starts to make a significant contribution in a QD. Values of e_{15} in the literature range from $e_{15} = -0.48$ to $e_{15} = +0.35 \text{ C/m}^2$, leading to a difference in potential drop of 8.6% for the dots that we consider here with $f=0.38$. This emphasizes the need for further measurement and analysis to develop a reliable set of material parameters for the nitrides.

The Schrödinger equation for the triangular well potential in Fig. 1 can be solved exactly in terms of the Airy function $\text{Ai}(x)$, giving

$$\psi(z) = \mathcal{N} \times \begin{cases} \exp(\sqrt{\beta}\sqrt{V-E_z}z), & z \leq 0, \\ \mathcal{CAi}\left[\left(\frac{\beta}{e^2 F^2}\right)^{1/3} (eFz - E_z)\right], & z > 0, \end{cases} \quad (8)$$

where

$$C = \left\{ \text{Ai} \left[- \left(\frac{\beta}{e^2 F^2} \right)^{1/3} E_z \right] \right\}^{-1} \quad (9)$$

$\beta = 2m^*/\hbar^2$, V is the band offset, and \mathcal{N} is a normalization constant. (This is the hole wave function; for the electron, the potential is inverted, so $z \rightarrow h - z$.) The energy E_z is obtained from the boundary conditions, which yield the expression

$$\text{Ai} \left(- \frac{\beta^{1/3} E_z}{(eF)^{2/3}} \right) = \frac{(eF)^{1/3}}{\beta^{1/6} \sqrt{V - E_z}} \text{Ai}' \left(- \frac{\beta^{1/3} E_z}{(eF)^{2/3}} \right). \quad (10)$$

This must be solved numerically to get E_z . However, it can be seen from Eq. (10) that the dependence of the energy on dot size enters only through the slope F of the potential. Hence, if F is constant, then E_z is also constant, and so, from the analysis in the previous section, E_z does not change when the height is varied, provided the height to radius ratio f remains constant.

We are now able to determine the value of k for the radial potential by taking $\partial_z^2 \varphi(z)$ at the position at which the Airy function solution attains its maximum value, i.e., at

$$z = \frac{E_z}{eF} + \frac{A'_0}{(\beta eF)^{1/3}} \quad (11)$$

where $A'_0 = -1.018793$ is the first root of $\text{Ai}'(x)$. A linear expansion of k shows that, at fixed f , k has a $1/R^2$ dependence, meaning that the lateral confinement energy E_r will vary approximately as $1/R$ for fixed f . However, the axial confinement energy E_z is typically 1–2 orders of magnitude larger than E_r , so this dependence on R will be almost unnoticeable in the total exciton energy.

Now, the ground-state exciton energy X^0 is given by

$$X^0 = E_g^{QD} + E_z^e + E_z^h + E_r^e + E_r^h + J_{eh} - eFh \quad (12)$$

where E_g^{QD} is the band gap of the QD material, J_{eh} is the Coulomb interaction energy, and the label e (h) refers to the electron (hole). J_{eh} is also about 1–2 orders of magnitude smaller than E_z , so J_{eh} , E_r^e , and E_r^h are of minor significance for the general trends discussed here. With this in mind, it can be seen that the exciton energy X^0 decreases linearly with dot height h for a fixed height to radius ratio [Fig. 2(a), dashed line], and the slope of this dependence is simply the slope of the polarization field times the electronic charge, eF . Studies by Adelman *et al.*¹⁴ have shown that GaN/AlN dots tend to conserve the ratio of height to radius as they grow, which explains why this linear dependence is seen in experiments where no deliberate effort has been made to obtain a uniform aspect ratio of the dots.⁴

The solution of the Airy function approximation compares well with the solution of a numerical finite-difference model using a one-band effective mass approximation and the full expression for the potential [solid line in Fig. 2(a)], overestimating the energy by about 0.1 eV. The wave functions also show good agreement (Fig. 3), making the approximation suitable for estimating quantities such as oscillator strength and Coulomb interaction energies.

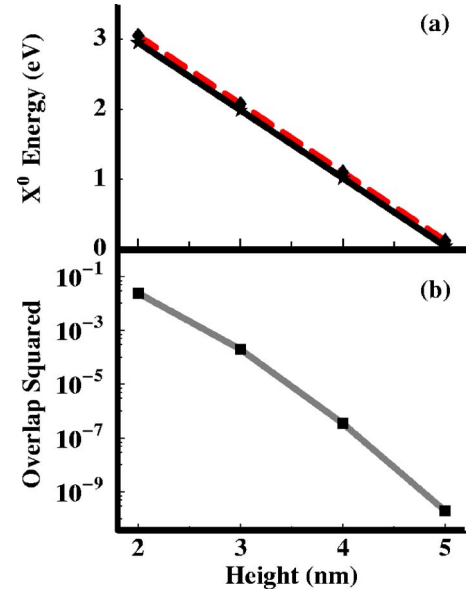


FIG. 2. (Color online) (a) Exciton energies as a function of dot height for cylindrical dots with $f=0.38$. Solid line, numerical calculation; dashed line, Airy function model. (b) Squared overlap of the electron and hole wave functions in each dot.

We can obtain an analytical expression for the energy if we make the further approximation $V \rightarrow \infty$, i.e., an infinite barrier. This gives

$$E_z = \frac{-A_0(eF)^{2/3}}{\beta^{1/3}} \quad (13)$$

where $A_0 = -2.33811$ is the first root of $\text{Ai}(x)$. This can be regarded as an upper bound for E_z . However, the wave functions are now a poor approximation since the infinite barrier forces the wave functions to be zero outside the dot, whereas in reality a significant portion of the wave function is non-zero outside the dot, as can be seen from Fig. 3. Similarly, we could improve the initial approximation by including a second finite potential step at the other side of the QD. A solution for this potential can also be found, but this now involves both Airy functions $\text{Ai}(x)$ and $\text{Bi}(x)$, and the equation for the energy is more complex than Eq. (10). Since the improvement in the accuracy of the energies and wave func-

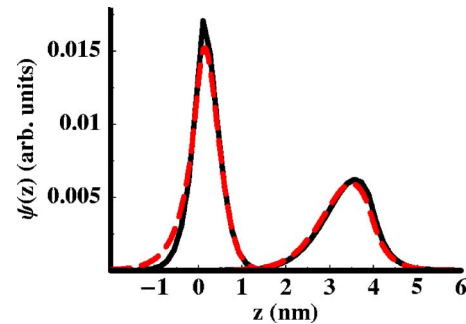


FIG. 3. (Color online) Hole (left) and electron (right) wave functions for the same 4-nm-high QD as Fig. 1. Solid lines, numerical calculation; dashed lines: Airy function wave functions.

tions is only very slight, the increased complexity makes this solution unhelpful for the current analysis.

The analysis presented here is for a single QD embedded in an infinite matrix. Many of the structures which have been studied experimentally contain multiple layers of dots, where the fields external to one dot (e.g., $z < 0$ nm and $z > 4$ nm in Fig. 1) can reduce the net field in neighboring dots. The spatial separation of the electron and hole wave functions caused by the polarization field will also lead to a self-screening effect, as described in the case of quantum wells by Di Carlo *et al.*¹⁵ This screening can be included self-consistently in more detailed studies of QDs.¹⁶ Fiorentini *et al.*¹⁷ also discuss a charge-density-dependent screening, and show that the total potential drop caused by the field will not be greater than the band gap energy. Figure 2(b) also confirms that the overlap of the electron and hole wave functions decreases rapidly with increasing dot size, suggesting that there will be little detectable photoluminescence from the ground state of larger dots. All these effects should be taken into account when comparing with experiment.

In conclusion, using analytical expressions that we have derived previously, we have shown that the built-in polarization potential in cylindrical nitride quantum dots is approximately linear in z along the central z axis of the dot for dots with a wide range of height to radius ratios, and we have presented an analytical expression for the slope of this po-

tential. We have shown that this slope depends only on the aspect ratio of the dot, and so will not change with dot size provided the aspect ratio is conserved. The approximation is also valid for truncated cone dots provided the side angle of the cone is sufficiently large. We have solved the Schrödinger equation for this approximate potential, and demonstrated analytically that the recombination energy of the ground-state exciton, X^0 , varies essentially linearly with dot height, again provided the aspect ratio f is held constant. Our analytical Airy function solution for the approximate potential shows very good agreement with the wave functions obtained from a one-band numerical calculation using the exact potential, confirming the validity and usefulness of the approximations used here when analyzing the electronic structure of GaN/AlN QDs. Finally we note that the uncertainty in the sign of the shear piezoelectric coefficient e_{15} (which has no consequence for quantum well structures), introduces a sizable uncertainty into the calculated magnitude of the potential in typical quantum dot structures, emphasizing the need for further measurement and analysis to develop a reliable value for this parameter.

We gratefully acknowledge support from Science Foundation Ireland and the Irish Research Council For Science, Engineering and Technology (D.P.W.).

*Email address: williams@tyndall.ie

¹M. Grundmann, O. Stier, and D. Bimberg, Phys. Rev. B **52**, 11969 (1995).

²T. Yamauchi, Y. Matsuba, L. Bolotov, M. Tabuchi, and A. Nakamura, Appl. Phys. Lett. **77**, 4368 (2000).

³M. A. Cusack, P. R. Briddon, and M. Jaros, Phys. Rev. B **54**, R2300 (1996).

⁴J. Simon, N. T. Pelekanos, C. Adelmann, E. Martinez-Guerrero, R. André, B. Daudin, L. S. Dang, and H. Mariette, Phys. Rev. B **68**, 035312 (2003).

⁵A. D. Andreev and E. P. O'Reilly, Phys. Rev. B **62**, 15851 (2000).

⁶D. P. Williams, A. D. Andreev, E. P. O'Reilly, and D. A. Faux, Phys. Rev. B **72**, 235318 (2005).

⁷I. Vurgaftman and J. R. Meyer, J. Appl. Phys. **94**, 3675 (2003).

⁸U. M. E. Christmas, A. D. Andreev, and D. A. Faux, J. Appl. Phys. **98**, 073522 (2005).

⁹S. Muensit, E. M. Goldys, and I. L. Guy, Appl. Phys. Lett. **75**, 3965 (1999).

¹⁰F. Bernardini and V. Fiorentini, Appl. Phys. Lett. **80**, 4145 (2002).

¹¹K. Tsubouchi and N. Mikoshiba, IEEE Trans. Sonics Ultrason. **32**, 634 (1985).

¹²G. Bu, D. Ciplis, M. Shur, L. J. Schowalter, S. Schujman, and R. Gaska, Appl. Phys. Lett. **84**, 4611 (2004).

¹³A. D. Andreev and E. P. O'Reilly, Appl. Phys. Lett. **79**, 521 (2001).

¹⁴C. Adelmann, B. Daudin, R. A. Oliver, G. A. D. Briggs, and R. E. Rudd, Phys. Rev. B **70**, 125427 (2004).

¹⁵A. Di Carlo *et al.*, Phys. Rev. B **63**, 235305 (2001).

¹⁶D. P. Williams, A. D. Andreev, and E. P. O'Reilly, Superlattices Microstruct. **36**, 791 (2004).

¹⁷V. Fiorentini, F. Bernardini, F. Della Sala, A. Di Carlo, and P. Lugli, Phys. Rev. B **60**, 8849 (1999).